



The Parathyroid Gland: An Overall Review of the Hidden Organ for Radiologists

부갑상선: 부갑상선 영상에 익숙하지 않은 영상의학과
의사들을 위한 전반적인 검토

Suho Kim, MD, Jung Hee Shin, MD*, Soo Yeon Hahn, MD,
Haejung Kim, MD, Myoung Kyoung Kim, MD

Department of Radiology, Samsung Medical Center, Sungkyunkwan University
School of Medicine, Seoul, Korea

Parathyroid glands are small endocrine glands that regulate calcium metabolism by producing parathyroid hormone (PTH). These are located at the back of the thyroid gland. Typically, four glands comprise the parathyroid glands, although their numbers may vary among individuals. Parathyroid diseases are related to parathyroid gland dysfunction and can be caused by problems with the parathyroid gland itself or abnormal serum calcium levels arising from renal disease. In recent years, as comprehensive health checkups have become more common, abnormal serum calcium levels are often found incidentally in blood tests, after which several additional tests, including a PTH test, ultrasonography (US), technetium-99m sestamibi parathyroid scan, single-photon-emission CT (SPECT)/CT, four-dimensional CT (4D-CT), and PET/CT, are performed for further evaluation. However, the parathyroid gland remains an organ less familiar to radiologists. Therefore, the normal anatomy, pathophysiology, imaging, and clinical findings of the parathyroid gland and its associated diseases are discussed here.

Index terms Parathyroid Gland; Ultrasonography; Tc-99m Sestamibi Scan; PET/CT

INTRODUCTION

The parathyroid glands produce the parathyroid hormone (PTH) to maintain serum calcium homeostasis. PTH stimulates the release of calcium and phosphate from the bone, reabsorbs calcium, inhibits phosphate reabsorption, stimulates calcitriol production in the kidney, and absorbs calcium in the bowel secondary to increased calcitriol levels (1). Diseases of the parathyroid gland are caused by either problems with

Received December 21, 2022

Revised June 15, 2023

Accepted August 8, 2023

*Corresponding author

Jung Hee Shin, MD

Department of Radiology,
Samsung Medical Center,
Sungkyunkwan University
School of Medicine,
81 Irwon-ro, Gangnam-gu,
Seoul 06351, Korea.

Tel 82-2-3410-2548

Fax 82-2-3410-2559

E-mail helena35@hanmail.net

This is an Open Access article distributed under the terms of the Creative Commons Attribution Non-Commercial License (<https://creativecommons.org/licenses/by-nc/4.0>) which permits unrestricted non-commercial use, distribution, and reproduction in any medium, provided the original work is properly cited.

Invited for the review at 2022
AOCR & KCR Annual Meeting.

the gland itself or abnormal serum calcium levels. Diagnosis is primarily based on clinical and biochemical methods. Recently, asymptomatic diagnoses have been made incidentally (2). As minimally invasive surgery has become mainstream, preoperative imaging-guided localization of parathyroid lesions and the role of radiologists have become more important (1, 3). In this study, we review the anatomy, pathophysiology, imaging, and clinical findings of the parathyroid gland.

ANATOMY

The average size of the parathyroid gland is 5 mm × 3 mm × 1 mm, and its weight is 35–40 mg (4). It is oval or bean-shaped and is usually composed of four endocrine glands (two superior and two inferior) in up to 81% of patients and fewer or more glands in 19% of patients (5). The superior gland is located posterior to the upper pole or interpolar area of the thyroid gland, whereas the inferior gland is located near the lower pole of the thyroid gland (6).

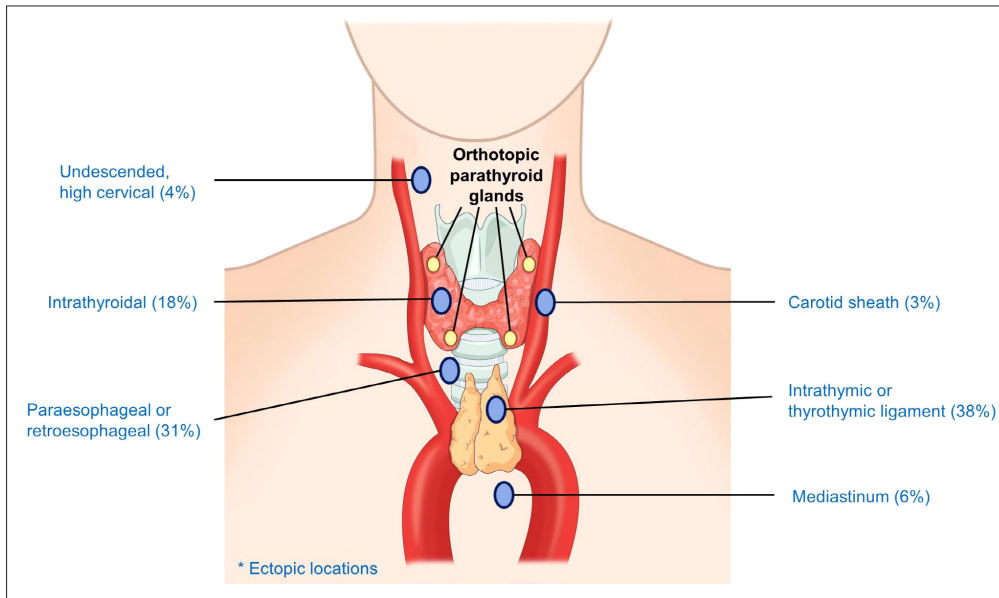
EMBRYOLOGY

The superior glands originate from the 4th branchial pouch with an ultimobranchial body. The dorsal wing of the 4th branchial pouch develops into the superior parathyroid glands, and the ventral wing differentiates into ultimobranchial bodies, which give rise to the parafollicular C-cells of the thyroid gland. The inferior glands derive from the 3rd branchial pouch of the thymus. The dorsal wing of the 3rd branchial pouch becomes the inferior parathyroid gland. The thymus also originates from the ventral wing of the 3rd branchial pouch. The inferior glands are initially cranial to the superior glands and migrate caudally over a greater distance, leading to a greater propensity for ectopic location (7).

ECTOPIC LOCATION

Aberrant migration can cause ectopic parathyroid glands with a prevalence of 16% in patients with primary hyperparathyroidism (Fig. 1) (5). The ectopic parathyroid glands are located between the angles of the mandible and mediastinum. Ectopic inferior parathyroid glands have greater variation and are most frequently located in the thymus (intrathymic) (30%), followed by the anterosuperior mediastinum (22%), intrathyroidal (22%), thyrothymic ligament (17%), and submandibular locations (8). Ectopic superior parathyroid glands are rare. They are most commonly found in the tracheoesophageal groove (43%), followed by the retroesophageal area (22%), posterosuperior mediastinum (14%), intrathyroidal area, and carotid sheath (9). The three most common ectopic locations are the thymus (38%), para- or retroesophageal space (31%), and thyroid (18%) (10). The ectopic gland could be one of the four parathyroid glands or a supernumerary gland. The recurrent laryngeal nerve is an important surgical landmark that helps differentiate between the superior and inferior parathyroid glands. The superior glands are located posteriorly to the plane of the recurrent laryngeal nerve within the tracheoesophageal groove, whereas the inferior glands are located anteriorly to this plane (11).

Fig. 1. Schematic of orthotopic and ectopic parathyroid glands, with ectopic parathyroid adenomas most commonly located in the thymus, paraesophageal or retroesophageal space, and the thyroid.



HISTOLOGY

The parathyroid gland is composed of chief cells, oxyphil cells, stromal fat, and connective tissue septa with a thin fibrous capsule. Chief cells are functional cells responsible for the synthesis and secretion of PTH and are more numerous than oxyphil cells. The function of oxyphil cells is unclear and no secretory granules are present in these cells. They are larger than the chief cells and scattered throughout the parathyroid gland. They have an eosinophilic cytoplasm due to their rich mitochondrial content (12). The average percentage of stromal fat is $35\% \pm 19\%$ and correlates with age, obesity grade, and serum PTH levels (13).

DISEASE OF THE PARATHYROID GLAND

Hyperparathyroidism is a condition characterized by high serum PTH levels. Primary hyperparathyroidism refers to hyperfunction of the parathyroid gland with high levels of PTH and calcium and normal or low levels of phosphate in the serum (1). Compensatory stimulation of the parathyroid gland for hypocalcemia results in secondary hyperparathyroidism with high PTH, low calcium, and varying phosphate levels. Chronic renal failure is the most common cause of this condition. In patients with long-term chronic renal failure, the loss of negative feedback leads to autonomous secretion of PTH, causing tertiary hyperparathyroidism with high PTH, calcium, and phosphate levels (2).

WHO CLASSIFICATION OF PARATHYROID TUMORS

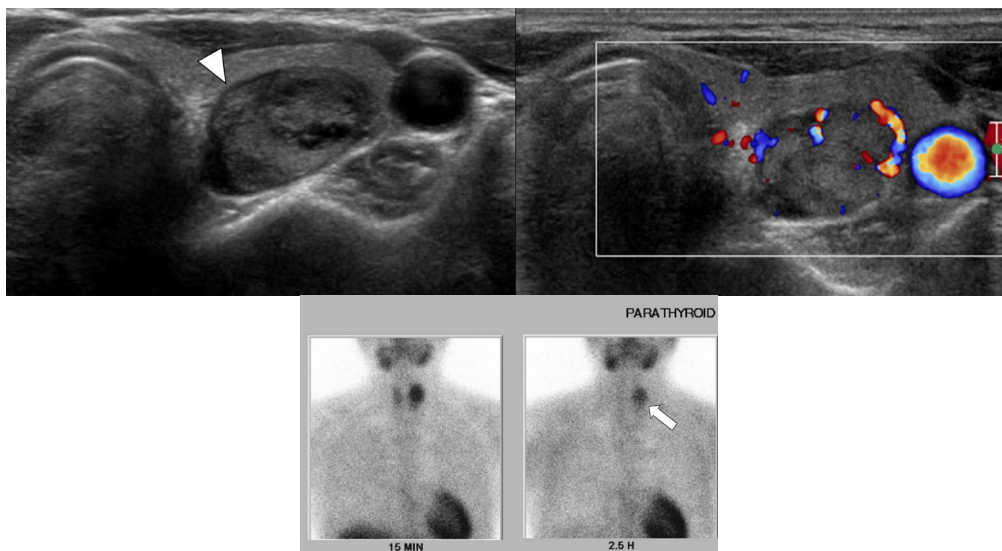
Parathyroid neoplasms can be classified into parathyroid adenomas, atypical parathyroid tumors, and parathyroid carcinomas. The term atypical parathyroid adenoma is no longer

used because of its uncertain malignant potential and has been replaced with the term atypical parathyroid tumor (Fig. 2) (14). Parathyroid hyperplasia has traditionally been considered as primary hyperparathyroidism that involves multiple parathyroid glands. However, the affected glands are usually composed of multiple clonal neoplastic proliferations in multiglandular primary hyperparathyroidism. Therefore, multiglandular parathyroid adenoma (primary hyperparathyroidism-related multiglandular diseases) is a more appropriate term than parathyroid hyperplasia, which is now used to refer to secondary hyperparathyroidism (14). Multiglandular parathyroid adenomas can have germline susceptibility, and genetic testing may be helpful in identifying underlying abnormalities, such as multiple endocrine neoplasia (MEN) types 1, 4, or 5. The absence of nuclear parafibromin (PFIB) immunoreactivity suggests a risk of tumor recurrence and an underlying germline or somatic CDC73 gene mutation with a high risk of parathyroid carcinoma. In patients with atypical parathyroid tumors, parathyroid carcinomas, and young patients with parathyroid adenomas and multiple other tumors, PFIB immunohistochemistry is helpful for further evaluation (14).

ULTRASONOGRAPHY

Currently, the most commonly used imaging modalities are ultrasonography (US) and technetium-99m sestamibi planar scintigraphy MIBI with additional single-photon emission CT (SPECT)/CT. Parathyroid US is an inexpensive and readily available imaging modality that does not use ionizing radiation. This offers the advantage of the concurrent evaluation of the thyroid gland. Normal parathyroid glands are not well visualized using conventional imaging. However, when visualized, they appear as hyperechoic structures with homogeneous echogenicity in 91% of cases and isoechoic structures with homogeneous echogenicity in 9%

Fig. 2. Atypical parathyroid tumor at the left superior parathyroid gland in a 60-year-old female with primary hyperparathyroidism: transverse and color Doppler US images show a 1.5 cm-sized heterogeneous iso- to hypoechoic mass (arrowhead) with a polar vessel sign at the posterior aspect of the left thyroid gland, while the ^{99m}Tc -MIBI scan shows a lesion with residual tracer uptake (arrow) in the left thyroid gland.

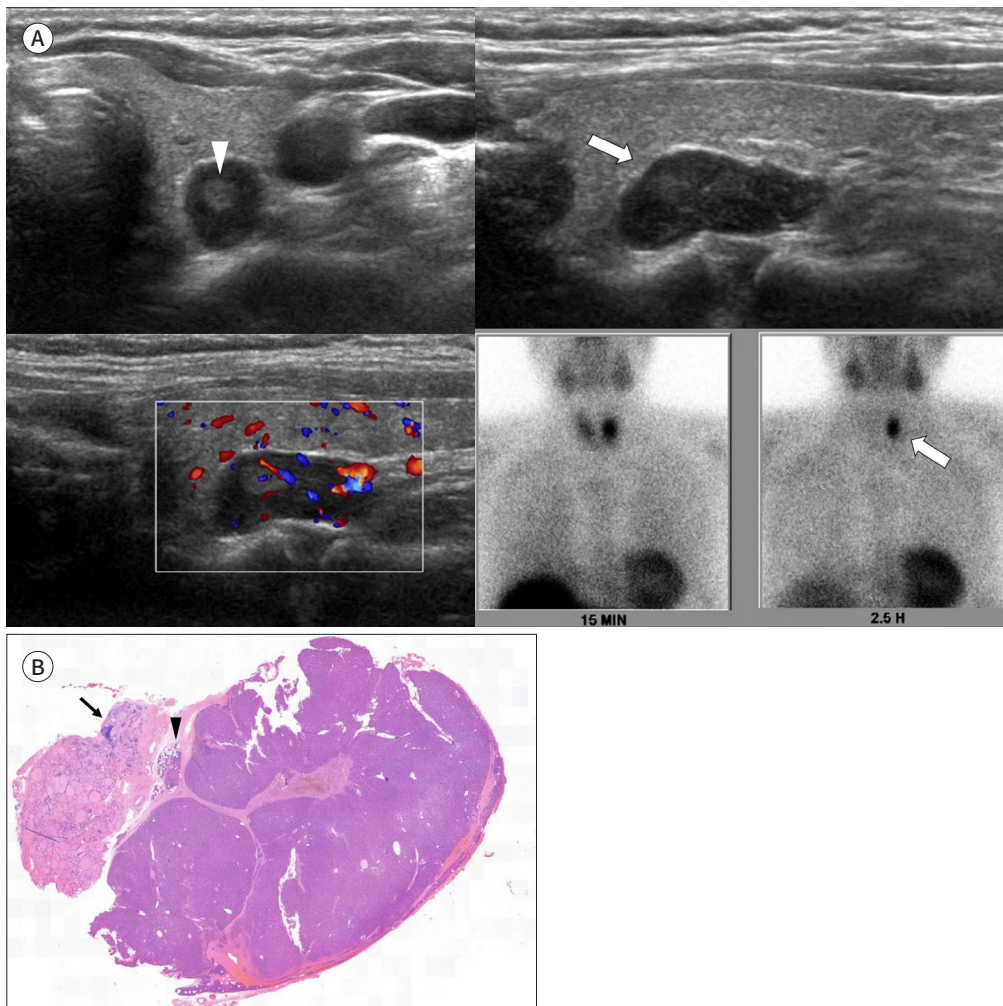


(15). Another recent study identified homogeneous hyperechogenicity with a circumscribed oval shape as a characteristic of the parathyroid gland (16). The stromal fat component of the parathyroid gland accounts for hyperechogenicity (17), whereas perithyroidal fat tissue can be distinguished by ill-defined margins and heterogeneous echotexture (16). Parathyroid adenomas are typically homogeneously hypoechoic relative to the thyroid gland, with a well-defined hyperechoic capsule or rim. The presence of residual normal parathyroid glands in the lesion can be observed in some cases with hyperechoic areas, which are defined as residual parathyroid signs (Fig. 3) (15). Parathyroid adenomas are oval or bean-shaped and when large are infrequently multilobulated. Hypervascularity in Doppler imaging due to feeding

Fig. 3. Solitary adenoma at the left inferior parathyroid gland in a 63-year-old female with primary hyperparathyroidism.

A. Transverse, sagittal and color doppler US images show a markedly hypoechoic nodule (arrow) with residual parathyroid sign (arrowhead) and polar vessel sign at the posterior aspect of the left thyroid lower pole, and ^{99m}Tc -MIBI scan shows a lesion (arrow) with residual uptake of the tracer in the region of the left thyroid gland.

B. Histopathology reveals a well-circumscribed mass with thin fibrous capsule and reduced stromal adipocytes (hematoxylin and eosin stain) attached to the thyroid tissue (arrow). Compressed nonneoplastic parathyroid tissue (arrowhead) containing 40%–50% fat component is seen at the edge, possibly corresponding to the residual parathyroid sign at US.

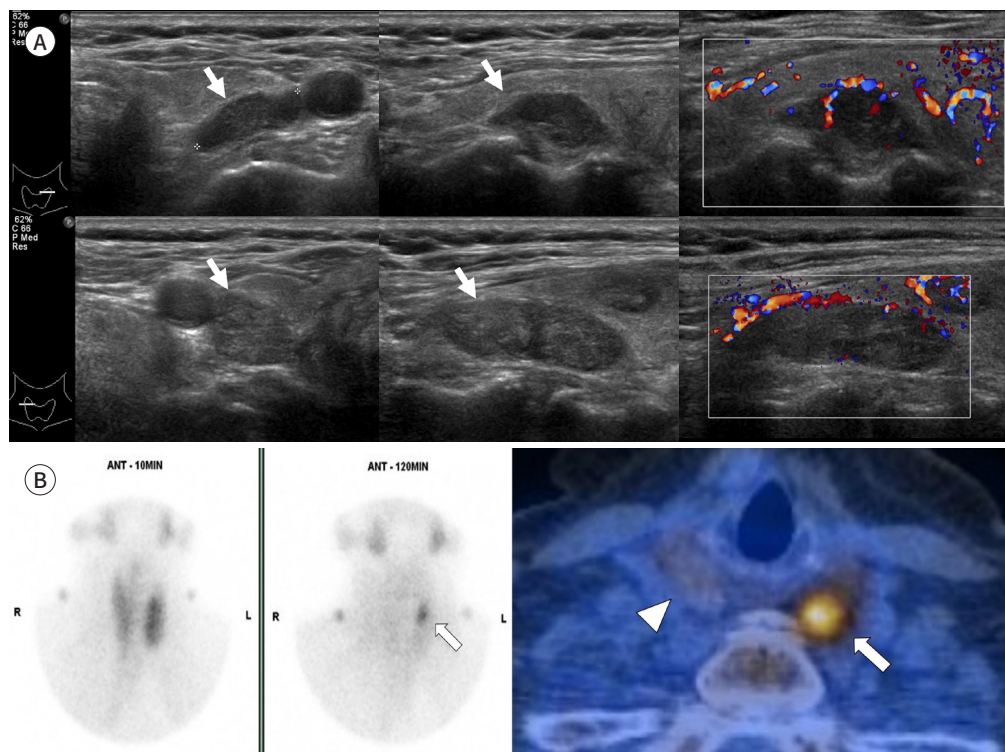


vessels is a characteristic of parathyroid adenoma and is known to feed the polar artery or vascularity along the peripheral rim (18). However, when adenomas are small and located deep within the tissue, they may not exhibit detectable blood flow on imaging (19). Less common features include cystic degeneration, hemorrhage, calcification, fibrosis, and fat deposition, resulting in a heterogeneous appearance and areas of increased echogenicity (8). Lymph nodes can be differentiated based on typical sonographic findings, such as hilar blood supply, hypoechoic cortex, and echogenic hilum. Exophytic thyroid nodules or separate thyroid lobulations, such as the tubercle of Zuckerkindl, may mimic parathyroid adenomas because of the thin hyperechoic septum between them and the thyroid gland. However, careful examination of the entire margin of the nodule can help to differentiate it by identifying the thin portion communicating with the thyroid gland (19). MIBI scanning or SPECT/CT is also helpful in differentiating thyroid lesions that mimic parathyroid adenomas on US (Fig. 4). Parathyroid carcinomas can cause severe hypercalcemia and require surgical treatment. The US features of parathyroid carcinomas (Fig. 5) include large size (mean, 3.5 cm), irregular shape, non-circumscribed margins, hypoechogenicity with heterogeneous echotexture, cystic change (13%–30%), calcification (10%–43%), infiltrative margin (50%–57%), and

Fig. 4. Solitary adenoma with misinterpreted ultrasonography in an 82-year-old female with primary hyperparathyroidism.

A. Transverse, sagittal and color doppler US images show hypoechoic masses (arrows) with peripheral vascularity at the posterior aspect of the both thyroid upper poles, which were initially thought to be parathyroid lesions.

B. ^{99m}Tc -MIBI scan shows a lesion (arrow) with residual uptake of the tracer in the region of the left thyroid gland; ^{11}C -methionine PET/CT also shows hot uptake (arrow) at the posterosuperior aspect to the left thyroid upper pole, but no uptake (arrowhead) at the right upper pole. The right lesion is a thyroid lesion.

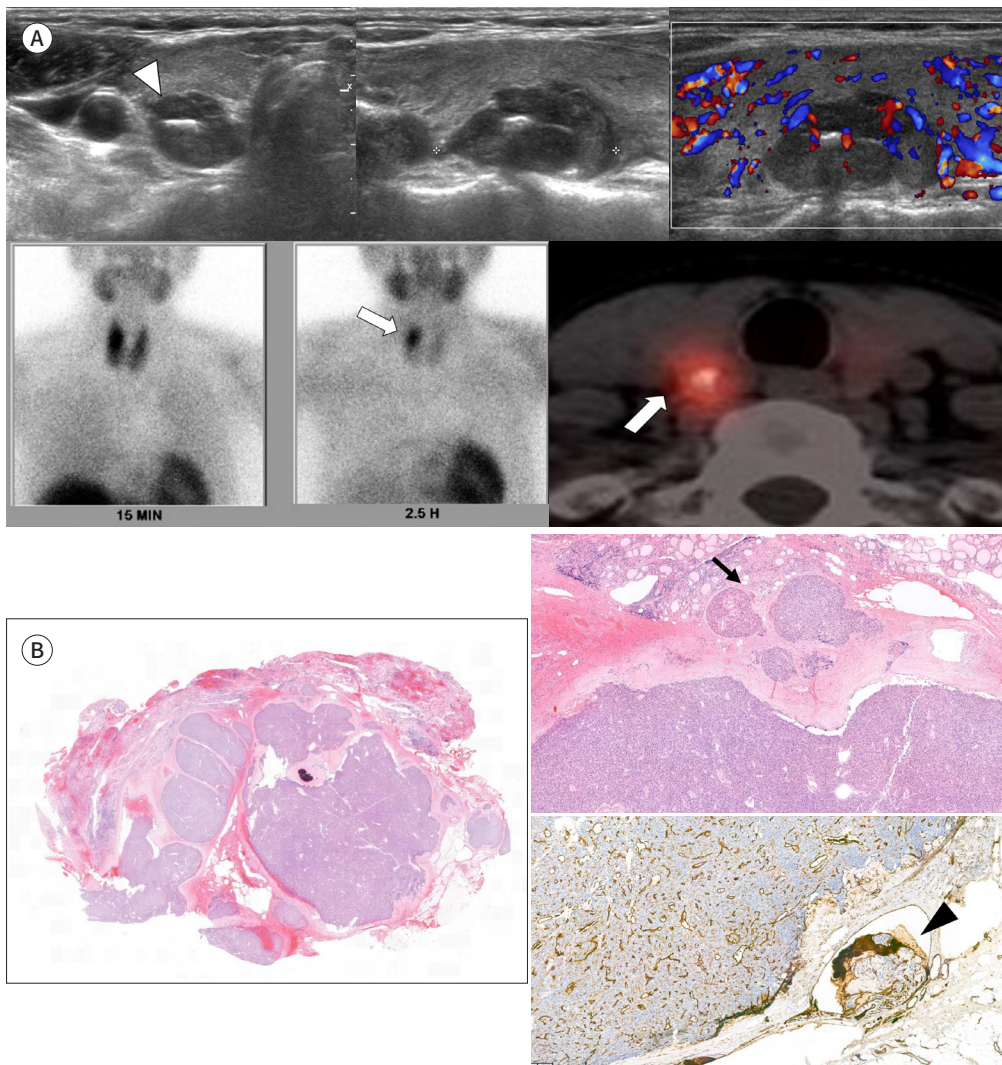


suspicious metastatic lymph nodes (14%) (20-22). US-guided fine needle aspiration (FNA) or biopsy with PTH washout analysis is recommended only for inconclusive or repeat surgical cases, such as ectopic locations, due to complications such as hematoma, post-FNA fibrosis, and risk of seeding in cases of parathyroid carcinoma. Fine-gauge needles (25–27 gauge) with gentle and fewer passes are recommended (23, 24). US-guided percutaneous ablation can be used as an alternative treatment option for parathyroid adenomas when primary or repeat parathyroidectomy is infeasible. It can also be considered for symptomatic secondary hyperparathyroidism that does not respond to medication and cannot be treated with surgery (25, 26).

Fig. 5. Parathyroid carcinoma at the right superior parathyroid gland in a 64-year-old female with primary hyperparathyroidism.

A. Transverse, sagittal and color doppler US images show a hypoechoic mass (arrowhead) with irregular margin, internal echogenic calcification and increased vascularity at the posterior aspect of the right thyroid mid-pole, ^{99m}Tc-MIBI scan shows a lesion (arrow) with prolonged uptake of the tracer in the region of the right thyroid gland, and ^{99m}Tc-MIBI SPECT/CT shows hot uptake and calcification in the lesion (arrow).

B. Histopathology shows a poorly circumscribed, multilobular mass with invasion of thyroid gland (arrow) (hematoxylin and eosin stain) and vascular invasion (arrowhead) on immunohistochemical staining for CD31.



4D-CT

Four-dimensional CT (4D-CT) has become the first line of study at several international institutions (27). The term 4D-CT refers to the number of phases and changes in perfusion over time (fourth dimension). A systematic review of 34 studies concluded that a three-phase protocol with pre-contrast imaging, an arterial phase (25–40 seconds), and a delayed venous phase (60–80 seconds) is the best for balancing diagnostic performance with radiation exposure. The late delayed phase (120 seconds) is no longer considered necessary (28). In non-contrast images, parathyroid adenomas and hyperplastic glands have low attenuation, while thyroid glands have high attenuation owing to their high iodine content. There are variable enhancement patterns of parathyroid adenomas, such as peak arterial enhancement greater than the thyroid gland with washout in the delayed phase (classic pattern), a lower degree of arterial enhancement than the thyroid gland but greater washout during the delayed phase (most common pattern), or similar enhancement and washout to the thyroid gland in a small proportion (29). Therefore, excluding the non-contrast phase from the imaging protocol may result in missing parathyroid lesions that appear similar to thyroid tissue in the arterial and venous phases. Cystic changes and intralesional hemorrhages can contribute to atypical enhancement. Thyroid tissue and lymph nodes show progressive enhancement for up to 90 seconds. Polar vessels are identified in up to two-thirds of cases, and an asymmetrically prominent vessel may guide clinicians to this abnormality (30). 4D-CT is not as widely used as US and MIBI scans for the initial evaluation of parathyroid lesions. However, it can be useful for anatomical localization in cases of persistent or recurrent hyperparathyroidism after surgery because of their adhesive and distorted architecture at the surgical site (31).

^{99m}Tc SESTAMIBI PLANAR SCINTIGRAPHY (MIBI SCAN)

Technetium-99m sestamibi (^{99m}Tc-MIBI) accumulates in mitochondria-rich cells, including the overactive parathyroid glands, myocardium, and malignant cells. Uptake is related to the oxyphil cell content of the parathyroid gland (18, 32). Dual-phase imaging with a single radiotracer or single-phase imaging with a dual radiotracer has been used to detect parathyroid lesions. In the dual-phase single-tracer protocol using ^{99m}Tc-MIBI, parathyroid adenomas show increased and prolonged tracer uptake in the delayed phase compared with the thyroid gland, which shows tracer washout, typically within 30 minutes (33). Approximately 700–1100 MBq of ^{99m}Tc-MIBI is administered in a dual-phase imaging protocol with a large field of view from the skull base to the diaphragm to detect ectopic tissue. Early- and delayed-phase images are acquired 10–30 minutes and 90–150 minutes, respectively, after administration of the radiopharmaceutical agent. Planar scintigraphy is performed at both time points, and SPECT/CT is commonly supplemented with delayed-phase imaging of MIBI scans because of its more precise anatomical localization (23, 34). Technetium-99m tetrofosmin (^{99m}Tc-TETRA) is an alternative radiotracer with parathyroid uptake. It has comparable imaging characteristics and the choice of agent depends on availability and experience of the interpreting physician (33). In dual-tracer single-phase protocol, radiotracer with parathyroid uptake (^{99m}Tc-MIBI or ^{99m}Tc-TETRA). These agents have comparable imaging characteristics, and the choice of the

agent depends on their availability and the experience of the interpreting physician (33). In the dual-tracer single-phase protocol, radiotracers with parathyroid uptake (^{99m}Tc or ^{99m}Tc -TETR) and a radiotracer without parathyroid uptake (^{99m}Tc -pertechnetate or I-123) are used. All these tracers accumulate in the functioning thyroid, and the subtraction of pertechnetate or iodine data from sestamibi or tetrofosmin data generates a parathyroid-only image (33, 34). This technique has been reported to have high sensitivity in detecting multiglandular diseases (23). In a single-tracer protocol, approximately 15% of parathyroid lesions, particularly hyperplastic glands, may demonstrate rapid washout of the radiotracer, similar to the washout pattern observed in the thyroid gland during MIBI scan (34). Furthermore, patients with thyroid disease or a history of thyroid surgery may show slower washout of the radiotracer from the thyroid gland than the typical washout rate in the single-tracer protocol. The differentiation between parathyroid lesions and thyroid tissues can be challenging in such cases. Subtraction techniques using dual-tracer protocols can potentially overcome these limitations but also have a higher radiation burden and are technically challenging (19, 23).

PET/CT

PET/CT has recently been accepted as an effective imaging modality for tumor localization. Several radiotracers have been used in PET/CT, including ^{11}C -methionine, ^{11}C -choline, and ^{18}F -fluorocholine. The detection rate of ^{18}F -fluorodeoxyglucose is inferior to those of ^{11}C -methionine and ^{18}F -choline (35). However, that study had a selection bias. Methionine is an essential amino acid precursor to PTH. However, it is not routinely used owing to its high cost and limited availability (23). Choline is an essential component of cell membrane metabolism that accumulates in overactive parathyroid cells. The widespread use of ^{11}C -labelled tracers is limited by their short half-life (approximately 20 minutes), which makes their transportation from centers with cyclotrons challenging. ^{18}F -choline is more suitable for clinical imaging than ^{11}C -choline owing to its longer half-life of 110 minutes, and it provides lower positron energies that result in less noise and offers improved spatial resolution (36). ^{18}F -choline PET/CT offers the highest sensitivity (90%) among available imaging modalities. It provides higher spatial resolution and shorter scanning time, requires a lower dose of radiation, but is more expensive than SPECT/CT. Therefore, it is an effective second-line tool for problematic cases with negative or discordant results on conventional imaging (Fig. 6) (37). The optimal ^{18}F -choline PET/CT protocol remains unclear. However, relying on single-time-point imaging, either in the early or late phases, carries a potential risk of missing lesions (23, 38). In dual-time point imaging, early and late images are usually acquired at 5–15 minutes and 45–60 minutes, respectively (39). Parathyroid adenomas usually exhibit more intense radiotracer uptake than the thyroid glands. The parathyroid to thyroid uptake ratio tends to be higher in late imaging because of faster washout of the radiotracer from the thyroid gland (23, 38).

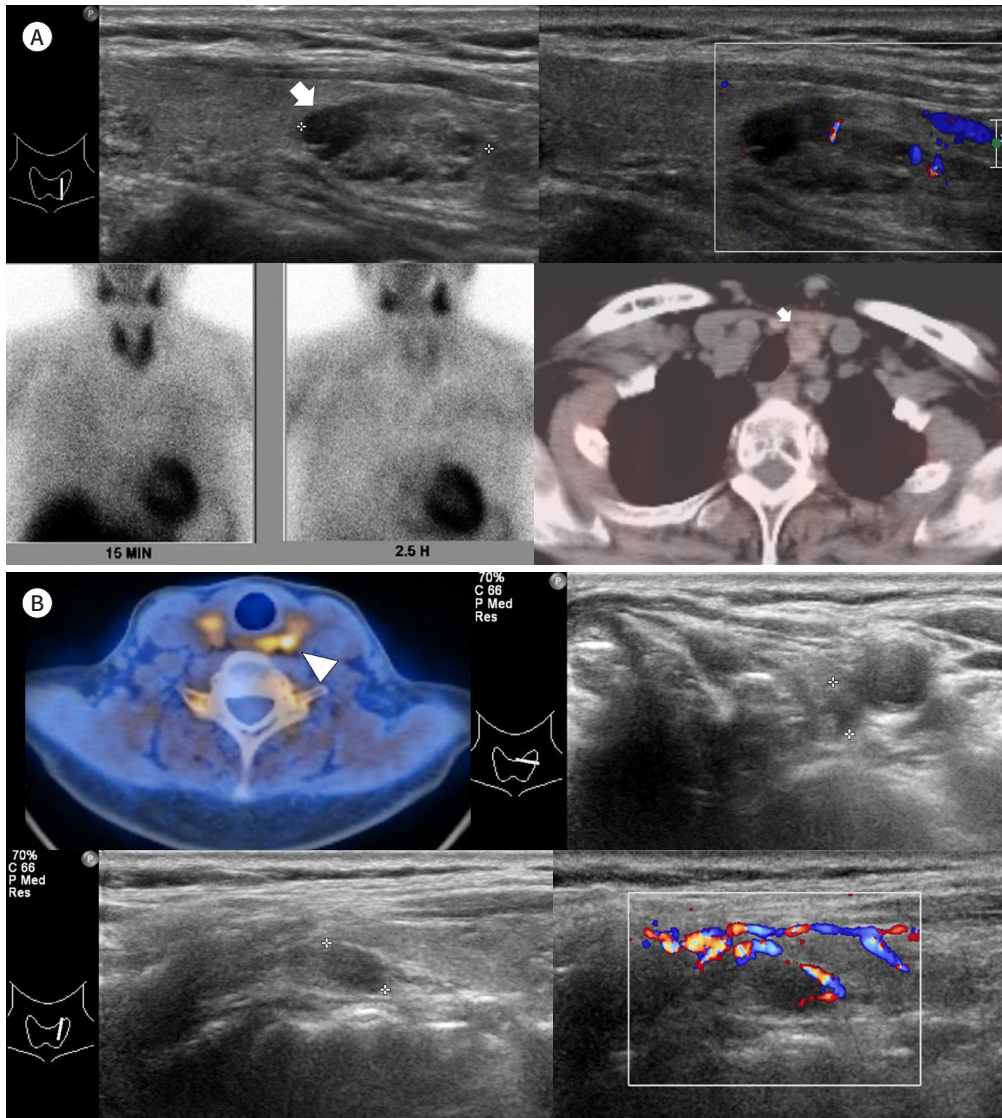
DIAGNOSTIC PERFORMANCE OF IMAGING MODALITIES

Several meta-analyses have compared the pooled sensitivity and positive predictive value (PPV) of parathyroid imaging techniques. In patients with primary hyperparathyroidism, the

Fig. 6. Solitary adenoma with false-negative US, MIBI scan and SPECT/CT in a 69-year-old female with primary hyperparathyroidism.

A. US images show a partially cystic isoechoic mass (arrow) with scanty flow signals at the inferior aspect of the left thyroid gland; ^{99m}Tc -MIBI scan and ^{99m}Tc SPECT/CT are negative with no tracer uptake, whereas non-enhanced CT shows a high attenuated mass (arrow) in the left thyroid gland.

B. ^{11}C -methionine PET/CT shows a nodular lesion (arrowhead) with hot uptake at the posterior aspect of the left thyroid gland upper pole, and US images reveal an oval marked hypoechoic mass (crosses) with a feeding vessel at the posterosuperior aspect to the left thyroid upper pole.



pooled sensitivity and PPV were 76% and 93% for US and 79% and 91% for ^{99m}Tc sestamibi SPECT, respectively (40). The sensitivity of combined scintigraphy and US ranges from 74% to 95% (1, 18). Therefore, US and MIBI complement each other as first-line modalities. The combination of SPECT or SPECT/CT with MIBI is a widely used technique.

Conventional imaging modalities (US, MIBI with SPECT, and SPECT/CT) remain insensitive to the detection of multiglandular disease in primary hyperparathyroidism. The detection rate of multiglandular disease is low for both US (16%–35%) and MIBI scan (30%–44%), show-

ing lower sensitivity compared with that for a solitary adenoma (41). Even with combined US and MIBI scans, the sensitivity ranges from 30% to 60% (18). Furthermore, 4D-CT and sestamibi SPECT/CT did not significantly improve the detection rate of multiglandular disease, with 58% in 4D-CT and 31% in SPECT/CT (42). However, ^{18}F -choline PET/CT showed a sensitivity of 91% and a specificity of 100%, demonstrating superior performance compared with conventional imaging methods (43, 44). It is now recognized that the time has come for ^{18}F -choline PET/CT to replace parathyroid planar scintigraphy. US still plays a role in preoperative localization or correlation with PET/CT.

PRIMARY HYPERPARATHYROIDISM

Autonomous PTH overproduction by abnormal parathyroid glands leads to primary hyperparathyroidism. Routine biochemical testing has increased the number of asymptomatic patients. The incidence of primary hyperparathyroidism varies between 0.4–82.0 cases per 100000 individuals, with sporadic cases in 95%, and familial syndromes in 5% (e.g., MEN1, MEN2A, MEN4, and familial isolated hyperparathyroidism). Ionizing radiation and chronic lithium therapy are the known risk factors (2). Genetic counselling is recommended for patients younger than 40 years with multiglandular disease or a family history. Primary hyperparathyroidism manifests as musculoskeletal diseases, recurrent urinary calculi, gastrointestinal dysfunction, and neurocognitive/neuropsychiatric diseases. Surgery is required for all symptomatic patients with primary hyperparathyroidism and for asymptomatic patients who meet the surgical indications (Table 1) (3). Solitary adenomas, double/multiple adenomas, and parathyroid carcinomas account for 89%, 10%, and 1% of cases of primary hyperparathyroidism, respectively (41). Minimally invasive parathyroidectomy is widely accepted as an effective and minimally invasive surgical technique that uses preoperative imaging-guided localization of solitary adenomas. For minimally invasive parathyroidectomy, intraoperative PTH monitoring is recommended to determine whether further exploration or bilateral neck exploration is required (3).

PERSISTENT OR RECURRENT HYPERPARATHYROIDISM

Persistent primary hyperparathyroidism refers to the occurrence of hyperparathyroidism within six months of parathyroidectomy, whereas recurrent primary hyperparathyroidism is

Table 1. Surgical Indications of Primary Hyperparathyroidism in Asymptomatic Patients

Age < 50 years
Serum calcium level > 1.0 mg/dL above upper limit of normal range
24-hour urinary calcium excretion > 400 mg/day
Estimated glomerular filtration rate < 60 mL/min/1.73 m ²
Nephrolithiasis or nephrocalcinosis
Vertebral or fragility fracture
Dual-energy X-ray absorptiometry T-score ≤ -2.5

diagnosed when hyperparathyroidism reappears after six months. In these cases, reoperation carries an increased risk of complications including recurrent laryngeal nerve injury, permanent hypothyroidism, and treatment failure (45). The most common causes of persistent and recurrent primary hyperparathyroidism are failure to identify the pathological glands and unrecognized multiglandular diseases. Ectopic and supernumerary glands are frequently observed in patients with persistent or recurrent primary hyperparathyroidism. Therefore, most surgeons require two concordant results from imaging studies before considering a repeat operation to improve localization (46). According to a study involving patients with sporadic primary hyperparathyroidism, the risk of multiglandular disease was 31.6% with two negative results, 3.6% with one positive result, and 0.0% with two concordant positive results based on preoperative imaging findings of US and MIBI scans (47).

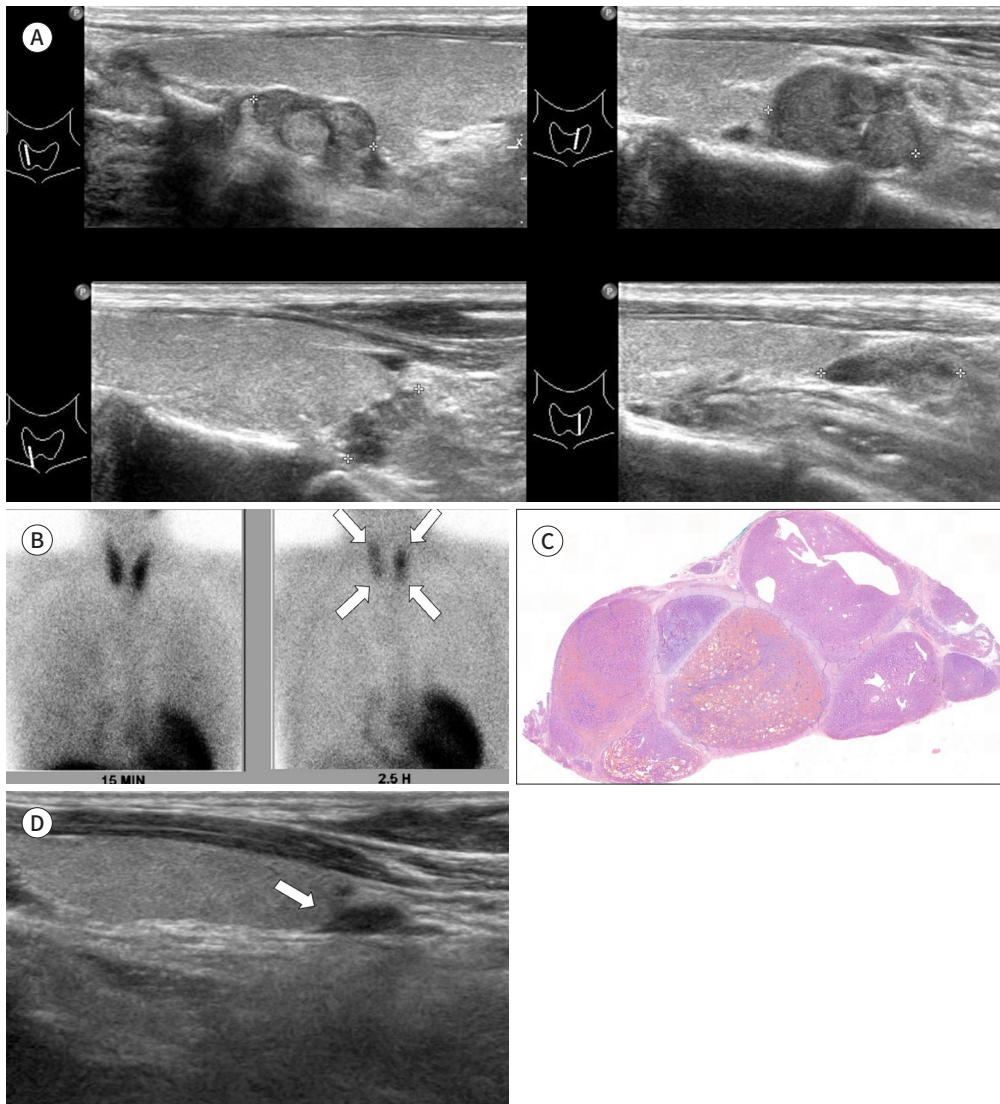
SECONDARY AND TERTIARY HYPERPARATHYROIDISM

Secondary hyperparathyroidism is caused by elevated PTH levels secondary to hypocalcemia, and can result from chronic renal failure or vitamin D deficiency. Tertiary hyperparathyroidism is characterized by the autonomous hyperfunction of the parathyroid gland in long-term secondary hyperparathyroidism due to the loss of feedback from serum calcium levels (1, 2). This condition can lead to hypercalcemia that may persist even after renal transplantation in patients with chronic renal failure (48). Medication is the mainstay treatment in secondary hyperparathyroidism. However, parathyroidectomy is required in patients with uncontrolled symptoms, such as bone pain, fracture, calciphylaxis, pruritus, and failure to correct metabolic parameters. In tertiary hyperparathyroidism, parathyroidectomy is the treatment of choice because it provides higher cure rates than medical management (49). Bilateral neck exploration is necessary to identify all four parathyroid glands. Total parathyroidectomy carries the risk of permanent hypoparathyroidism; therefore, total parathyroidectomy with autotransplantation and subtotal parathyroidectomy are often preferred (48, 49). The aim of preoperative imaging is to identify ectopic and supernumerary parathyroid glands and asymmetric gland hyperplasia, and to evaluate concurrent thyroid disease (50). The US features of secondary and tertiary hyperparathyroidism are similar to those of primary hyperparathyroidism, with well-defined hypoechoic lesions and peripheral vascularity. However, the incidence of mixed echogenicity, cystic changes, calcification, supernumerary glands, and ectopic parathyroid glands is higher than that in primary hyperparathyroidism (Fig. 7) (51, 52). ¹⁸F-choline PET/CT is reportedly more sensitive (86%) and accurate (87%) than US (62% and 65%, respectively) and sestamibi SPECT/CT (55% and 59%, respectively) in patients with secondary and tertiary hyperparathyroidism. It also offers the advantage of detecting intrathyroidal hyperfunctioning parathyroid glands, although false-positive results may occur because of benign and malignant thyroid nodules (50, 53).

PARATHYROID INCIDENTALOMA

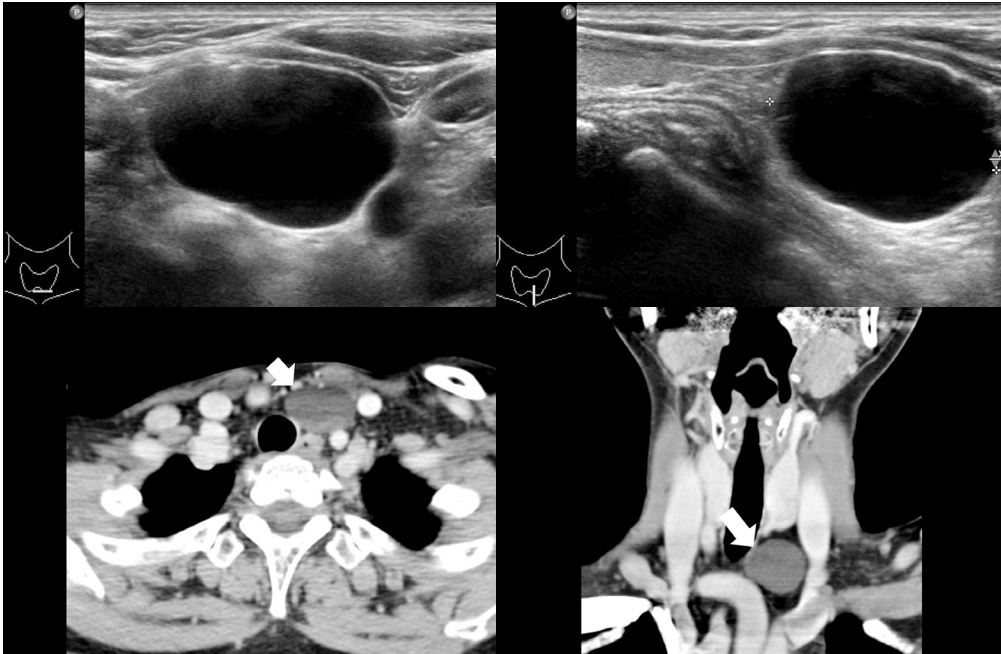
Parathyroid incidentaloma refers to unexpected parathyroid lesions detected incidentally during imaging or surgery. The incidence of parathyroid incidentaloma detected on US is

Fig. 7. Multiple hyperplasia of all four parathyroid glands in a 46-year-old male with tertiary hyperparathyroidism: sagittal US images (A) showing multiple masses (crosses) of variable size and mixed echogenicity in the posterior and inferior aspects of both thyroid glands, while ^{99m}Tc -MIBI scan (B) shows all four parathyroid lesions (arrows) with residual tracer uptake in both thyroid glands, histopathology (C) shows nodular growth without a definite rim of compressed normal parathyroid tissue (hematoxylin and eosin staining), and follow-up sagittal US image (D) after one year shows the preserved remaining left inferior parathyroid gland (arrow) at the inferior aspect of the left thyroid gland.



0.4%–1.2% (54, 55). Most incidentalomas are non-functioning or less functioning, and may represent an early stage of the development of primary hyperparathyroidism. The possibility of an enlarged parathyroid gland should be considered when a homogeneous, hypoechoic, well-defined oval nodule with a feeding vessel is found beyond the thyroid capsule (54, 55). If the imaging characteristics and location of an incidental lesion suggest an enlarged parathyroid gland, further clinical and biochemical assessments should be performed to evaluate the hyperfunctioning glands. Additional US-guided FNA with a PTH assay in the washout fluid can accurately diagnose parathyroid incidentalomas detected during thyroid US. For the de-

Fig. 8. Parathyroid cyst at the left inferior parathyroid gland in a 54-year-old female who presented with anterior neck swelling: US images show an anechoic cystic mass (cross) at the inferior aspect of the left thyroid gland, and neck CT images performed at other hospitals show a cystic mass (arrows) in the left infrathyroidal and paratracheal areas.



tection of incidentalomas, the PPV of thyroid US is 21.4%, and multinodular goiters or perithyroidal lymph nodes may account for false-positive diagnoses (55). Most patients with hyperfunctioning parathyroid incidentalomas are asymptomatic. Several factors, including serum and urinary calcium levels, renal function, and bone density, should be considered for appropriate management.

PARATHYROID CYST

A true parathyroid cyst is a nonfunctioning lesion, but if large, it can cause compressive symptoms (Fig. 8). Sung et al. (56) showed that the success rate of US-guided aspiration was only 33%. Ethanol ablation can be considered in recurrent cases (55-57). In contrast, functional parathyroid cysts and cystic parathyroid adenomas are suspected to originate from cystic degeneration and hemorrhage. Non-functioning parathyroid cysts have unilocular clear fluid, while cystic parathyroid adenomas have cloudy brown fluid, suggesting a previous hemorrhage (57, 58).

CONCLUSION

Several imaging modalities are available for preoperative localization of parathyroid tumors and hyperplasia. US and MIBI scans with SPECT/CT are the first modalities, whereas ^{18}F -choline PET/CT is used as the second modality in negative or discordant cases. 4D-CT can also serve as a problem-solving technique in challenging cases. To make an accurate diagnosis and

provide proper information before surgery, radiologists should be aware of the characteristic radiological findings and the overall management of parathyroid diseases.

Author Contributions

Conceptualization, all authors; data curation, all authors; formal analysis, all authors; funding acquisition, all authors; investigation, all authors; methodology, all authors; project administration, all authors; resources, all authors; software, all authors; supervision, all authors; validation, all authors; visualization, all authors; writing—original draft, all authors; and writing—review & editing, all authors.

Conflicts of Interest

The authors have no potential conflicts of interest to disclose.

ORCID iDs

Suho Kim  <https://orcid.org/0000-0003-1740-8216>

Jung Hee Shin  <https://orcid.org/0000-0001-6435-7357>

Soo Yeon Hahn  <https://orcid.org/0000-0002-4099-1617>

Haejung Kim  <https://orcid.org/0000-0003-4855-9711>

Myoung Kyoung Kim  <https://orcid.org/0000-0001-9228-022X>

Funding

None

Acknowledgments

Figure 1 was drawn by Da Hyeun Lee, Samsung Medical Information and Medical Services.

REFERENCES

1. Johnson NA, Carty SE, Tublin ME. Parathyroid imaging. *Radiol Clin North Am* 2011;49:489-509, vi
2. Walker MD, Silverberg SJ. Primary hyperparathyroidism. *Nat Rev Endocrinol* 2018;14:115-125
3. Wilhelm SM, Wang TS, Ruan DT, Lee JA, Asa SL, Duh QY, et al. The American Association of Endocrine Surgeons guidelines for definitive management of primary hyperparathyroidism. *JAMA Surg* 2016;151:959-968
4. Wang C. The anatomic basis of parathyroid surgery. *Ann Surg* 1976;183:271-275
5. Tattera D, Wong LM, Vikse J, Sanna B, Pękala P, Walocha J, et al. The prevalence and anatomy of parathyroid glands: a meta-analysis with implications for parathyroid surgery. *Langenbecks Arch Surg* 2019;404:63-70
6. Policeni BA, Smoker WR, Reede DL. Anatomy and embryology of the thyroid and parathyroid glands. *Semin Ultrasound CT MR* 2012;33:104-114
7. Grevellec A, Tucker AS. The pharyngeal pouches and clefts: development, evolution, structure and derivatives. *Semin Cell Dev Biol* 2010;21:325-332
8. Kuzminski SJ, Sosa JA, Hoang JK. Update in parathyroid imaging. *Magn Reson Imaging Clin N Am* 2018;26:151-166
9. Phitayakorn R, McHenry CR. Incidence and location of ectopic abnormal parathyroid glands. *Am J Surg* 2006;191:418-423
10. Roy M, Mazeh H, Chen H, Sippel RS. Incidence and localization of ectopic parathyroid adenomas in previously unexplored patients. *World J Surg* 2013;37:102-106
11. Mohebbati A, Shaha AR. Anatomy of thyroid and parathyroid glands and neurovascular relations. *Clin Anat* 2012;25:19-31
12. Grimelius L, Bondeson L. Histopathological diagnosis of parathyroid diseases. *Pathol Res Pract* 1995;191:353-365
13. Iwasaki A, Shan L, Kawano I, Nakamura M, Utsuno H, Kobayashi A, et al. Quantitative analysis of stromal fat content of human parathyroid glands associated with thyroid diseases using computer image analysis. *Pathol Int* 1995;45:483-486
14. Erickson LA, Mete O, Juhlin CC, Perren A, Gill AJ. Overview of the 2022 WHO classification of parathyroid

- tumors. *Endocr Pathol* 2022;33:64-89
15. Xia C, Zhu Q, Li Z, Hu M, Fang J, Zhong Q, et al. Study of the ultrasound appearance of the normal parathyroid using an intraoperative procedure. *J Ultrasound Med* 2019;38:321-327
 16. Paik W, Lee JC, Noh BJ, Na DG. US features of the parathyroid glands: an intraoperative surgical specimen study. *J Korean Soc Radiol* 2023;84:596-605
 17. Li J, Yang X, Chang X, Ouyang Y, Hu Y, Li M, et al. A retrospective study of ultrasonography in the investigation of primary hyperparathyroidism: a new perspective for ultrasound echogenicity features of parathyroid nodules. *Endocr Pract* 2021;27:1004-1010
 18. Johnson NA, Tublin ME, Ogilvie JB. Parathyroid imaging: technique and role in the preoperative evaluation of primary hyperparathyroidism. *AJR Am J Roentgenol* 2007;188:1706-1715
 19. Itani M, Middleton WD. Parathyroid imaging. *Radiol Clin North Am* 2020;58:1071-1083
 20. Fang C, Konstantatou E, Mulholland NJ, Baroncini S, Husainy MA, Schulte KM, et al. A retrospective review of the role of B-mode and color Doppler ultrasonography in the investigation of primary hyperparathyroidism: features that differentiate benign from malignant lesions. *Ultrasound* 2018;26:110-117
 21. Nam M, Jeong HS, Shin JH. Differentiation of parathyroid carcinoma and adenoma by preoperative ultrasonography. *Acta Radiol* 2017;58:670-675
 22. Liu J, Zhan WW, Zhou JQ, Zhou W. Role of ultrasound in the differentiation of parathyroid carcinoma and benign parathyroid lesions. *Clin Radiol* 2020;75:179-184
 23. Petranović Ovcariček P, Giovanella L, Carrió Gasset I, Hindié E, Huellner MW, Luster M, et al. The EANM practice guidelines for parathyroid imaging. *Eur J Nucl Med Mol Imaging* 2021;48:2801-2822
 24. Abraham D, Duick DS, Baskin HJ. Appropriate administration of fine-needle aspiration (FNA) biopsy on selective parathyroid adenomas is safe. *Thyroid* 2008;18:581-582; author reply 583-584
 25. Zhou X, Shen Y, Zhu Y, Lv Q, Pu W, Gao L, et al. Ultrasound-guided microwave ablation for secondary hyperparathyroidism: a systematic review and meta-analysis. *Int J Hyperthermia* 2021;38:1285-1294
 26. Hänsler J, Harsch IA, Strobel D, Hahn EG, Becker D. [Treatment of a solitary adenoma of the parathyroid gland with ultrasound-guided percutaneous radio-frequency-tissue-ablation (RFTA)]. *Ultraschall Med* 2002; 23:202-206. German
 27. Hoang JK, Williams K, Gaillard F, Dixon A, Sosa JA. Parathyroid 4D-CT: multi-institutional international survey of use and trends. *Otolaryngol Head Neck Surg* 2016;155:956-960
 28. Kluijfhout WP, Pasternak JD, Beninato T, Drake FT, Gosnell JE, Shen WT, et al. Diagnostic performance of computed tomography for parathyroid adenoma localization; a systematic review and meta-analysis. *Eur J Radiol* 2017;88:117-128
 29. Bahl M, Sepahdari AR, Sosa JA, Hoang JK. Parathyroid adenomas and hyperplasia on four-dimensional CT scans: three patterns of enhancement relative to the thyroid gland justify a three-phase protocol. *Radiology* 2015;277:454-462
 30. Bahl M, Muzaffar M, Vij G, Sosa JA, Choudhury KR, Hoang JK. Prevalence of the polar vessel sign in parathyroid adenomas on the arterial phase of 4D CT. *AJNR Am J Neuroradiol* 2014;35:578-581
 31. Zafereo M, Yu J, Angelos P, Brumund K, Chuang HH, Goldenberg D, et al. American Head and Neck Society Endocrine Surgery Section update on parathyroid imaging for surgical candidates with primary hyperparathyroidism. *Head Neck* 2019;41:2398-2409
 32. Stephen AE, Roth SI, Fardo DW, Finkelstein DM, Randolph GW, Gaz RD, et al. Predictors of an accurate preoperative sestamibi scan for single-gland parathyroid adenomas. *Arch Surg* 2007;142:381-386
 33. Smith JR, Oates ME. Radionuclide imaging of the parathyroid glands: patterns, pearls, and pitfalls. *RadioGraphics* 2004;24:1101-1115
 34. Greenspan BS, Dillehay G, Intenzo C, Lavelly WC, O'Doherty M, Palestro CJ, et al. SNM practice guideline for parathyroid scintigraphy 4.0. *J Nucl Med Technol* 2012;40:111-118
 35. Kluijfhout WP, Pasternak JD, Drake FT, Beninato T, Gosnell JE, Shen WT, et al. Use of PET tracers for parathyroid localization: a systematic review and meta-analysis. *Langenbecks Arch Surg* 2016;401:925-935
 36. Lalonde MN, Correia RD, Sykietitis GP, Schaefer N, Matter M, Prior JO. Parathyroid imaging. *Semin Nucl Med* 2023;53:490-502
 37. Kim SJ, Lee SW, Jeong SY, Pak K, Kim K. Diagnostic performance of F-18 fluorocholine PET/CT for parathyroid localization in hyperparathyroidism: a systematic review and meta-analysis. *Horm Cancer* 2018;9:440-447

38. Broos WAM, Wondergem M, van der Zant FM, Knol RJJ. Dual-time-point 18F-fluorocholine PET/CT in parathyroid imaging. *J Nucl Med* 2019;60:1605-1610
39. Uslu-Besli L, Sonmezoglu K, Teksoz S, Akgun E, Karayel E, Pehlivanoglu H, et al. Performance of F-18 fluorocholine PET/CT for detection of hyperfunctioning parathyroid tissue in patients with elevated parathyroid hormone levels and negative or discrepant results in conventional imaging. *Korean J Radiol* 2020;21:236-247
40. Cheung K, Wang TS, Farrokhyar F, Roman SA, Sosa JA. A meta-analysis of preoperative localization techniques for patients with primary hyperparathyroidism. *Ann Surg Oncol* 2012;19:577-583
41. Ruda JM, Hollenbeak CS, Stack BC Jr. A systematic review of the diagnosis and treatment of primary hyperparathyroidism from 1995 to 2003. *Otolaryngol Head Neck Surg* 2005;132:359-372
42. Yeh R, Tay YD, Tabacco G, Dercle L, Kuo JH, Bandeira L, et al. Diagnostic performance of 4D CT and sestamibi SPECT/CT in localizing parathyroid adenomas in primary hyperparathyroidism. *Radiology* 2019;291:469-476
43. Lezaic L, Rep S, Sever MJ, Kocjan T, Hocevar M, Fettich J. ¹⁸F-Fluorocholine PET/CT for localization of hyperfunctioning parathyroid tissue in primary hyperparathyroidism: a pilot study. *Eur J Nucl Med Mol Imaging* 2014;41:2083-2089
44. Treglia G, Piccardo A, Imperiale A, Strobel K, Kaufmann PA, Prior JO, et al. Diagnostic performance of choline PET for detection of hyperfunctioning parathyroid glands in hyperparathyroidism: a systematic review and meta-analysis. *Eur J Nucl Med Mol Imaging* 2019;46:751-765
45. Wells SA Jr, DeBenedetti MK, Doherty GM. Recurrent or persistent hyperparathyroidism. *J Bone Miner Res* 2002;17 Suppl 2:N158-N162
46. Udelsman R, Donovan PI. Remedial parathyroid surgery: changing trends in 130 consecutive cases. *Ann Surg* 2006;244:471-479
47. Sebag F, Hubbard JG, Maweja S, Misso C, Tardivet L, Henry JF. Negative preoperative localization studies are highly predictive of multiglandular disease in sporadic primary hyperparathyroidism. *Surgery* 2003;134:1038-1041; discussion 1041-1042
48. van der Plas WY, Noltjes ME, van Ginhoven TM, Kruijff S. Secondary and tertiary hyperparathyroidism: a narrative review. *Scand J Surg* 2020;109:271-278
49. Dream S, Kuo LE, Kuo JH, Sprague SM, Nwariaku FE, Wolf M, et al. The American Association of Endocrine Surgeons guidelines for the definitive surgical management of secondary and tertiary renal hyperparathyroidism. *Ann Surg* 2022;276:e141-e176
50. Chen YH, Chen HT, Lee MC, Liu SH, Wang LY, Lue KH, et al. Preoperative F-18 fluorocholine PET/CT for the detection of hyperfunctioning parathyroid glands in patients with secondary or tertiary hyperparathyroidism: comparison with Tc-99m sestamibi scan and neck ultrasound. *Ann Nucl Med* 2020;34:527-537
51. Alkhalili E, Tasci Y, Aksoy E, Aliyev S, Soundararajan S, Taskin E, et al. The utility of neck ultrasound and sestamibi scans in patients with secondary and tertiary hyperparathyroidism. *World J Surg* 2015;39:701-705
52. Mingkwansook V, Buranont C, Watcharakorn A. Ultrasonographic appearances of parathyroid gland hyperplasia in tertiary hyperparathyroidism. *J Med Assoc Thai* 2017;100:156
53. Xue Y, Li W, Xia Z, Lei C, Cao Y, Wang Z, et al. The role of 18F-FCH PET/CT in patients with uremic hyperparathyroidism compared with 99mTc-sestaMIBI SPECT/CT and ultrasonography. *EJNMMI Res* 2019;9:118
54. Ghervan C, Silaghi A, Nemeş C. Parathyroid incidentaloma detected during thyroid sonography - prevalence and significance beyond images. *Med Ultrason* 2012;14:187-191
55. Kwak JY, Kim EK, Moon HJ, Kim MJ, Ahn SS, Son EJ, et al. Parathyroid incidentalomas detected on routine ultrasound-directed fine-needle aspiration biopsy in patients referred for thyroid nodules and the role of parathyroid hormone analysis in the samples. *Thyroid* 2009;19:743-748
56. Sung JY, Baek JH, Kim KS, Lee D, Ha EJ, Lee JH. Symptomatic nonfunctioning parathyroid cysts: role of simple aspiration and ethanol ablation. *Eur J Radiol* 2013;82:316-320
57. Ippolito G, Palazzo FF, Sebag F, Sierra M, De Micco C, Henry JF. A single-institution 25-year review of true parathyroid cysts. *Langenbecks Arch Surg* 2006;391:13-18
58. Johnson NA, Yip L, Tublin ME. Cystic parathyroid adenoma: sonographic features and correlation with 99mTc-sestaMIBI SPECT findings. *AJR Am J Roentgenol* 2010;195:1385-1390

부갑상선: 부갑상선 영상에 익숙하지 않은 영상학과 의사들을 위한 전반적인 검토

김수호 · 신정희* · 한수연 · 김해정 · 김명경

부갑상선은 부갑상선 호르몬(parathyroid hormone; 이하 PTH)을 생성하여 칼슘 대사를 조절하는 작은 내분비선으로 구성되어 있다. 일반적으로 갑상선 뒤에 4개의 부갑상선이 위치해 있으나 개수 또는 위치는 개인차가 있으며 4개보다 많거나 적은 경우들이 있다. 부갑상선 질환은 부갑상선 기능 장애와 관련이 있으며, 부갑상선 자체의 문제 또는 신장질환으로 인한 비정상적인 혈청 칼슘 수치로 인해 발생할 수 있다. 최근 건강검진이 보편화되면서 우연히 비정상적으로 높은 혈청 칼슘 값이 발견되어 PTH 검사, 초음파, 테크네튬-99m 세스타미비 부갑상선 스캔, 단일광자방출단층촬영/컴퓨터단층촬영(SPECT/CT), 4차원 컴퓨터단층촬영(4D-CT), 그리고 양전자방출단층촬영/컴퓨터단층촬영(PET/CT) 등의 추가적인 검사가 시행된다. 그러나 부갑상선은 여전히 영상학과 의사에게 익숙하지 않은 기관이다. 이 종설에서 부갑상선의 해부학, 병태생리, 영상 및 임상 소견에 대해 알아보려고 한다.

성균관대학교 의과대학 삼성서울병원 영상학과